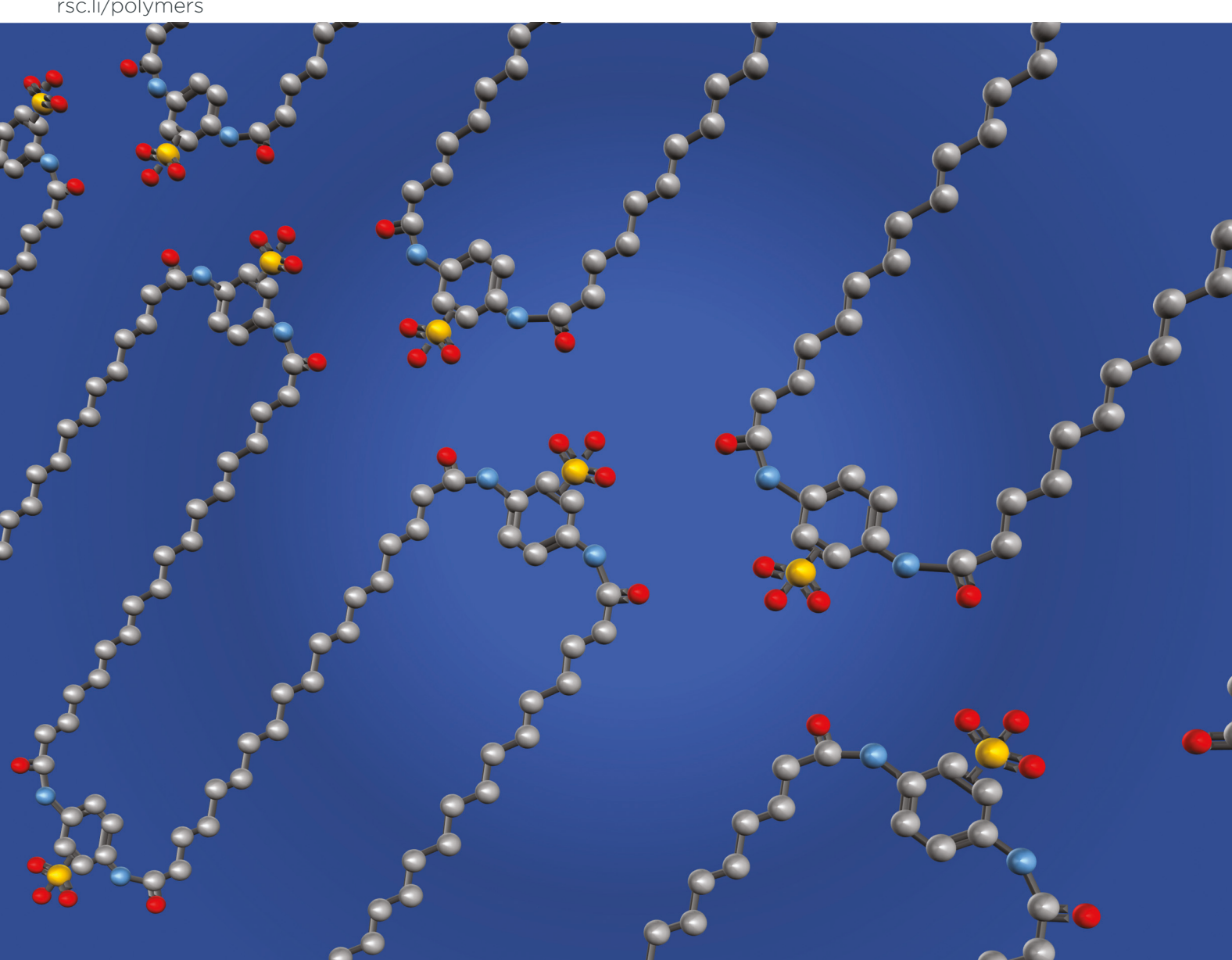
Volume 13 Number 41 7 November 2022 Pages 5791-5932

Polymer Chemistry

rsc.li/polymers



ISSN 1759-9962



PAPER

Polymer Chemistry



PAPER View Article Online
View Journal | View Issue



Cite this: *Polym. Chem.*, 2022, **13**, 5811

Nanoscale layers of precise ion-containing polyamides with lithiated phenyl sulfonate in the polymer backbone†

Jinseok Park, ¹

a Charles P. Easterling, ¹

b Christopher C. Armstrong,

Charles P. Easterling, ¹

Christopher C. Armstrong,

Karen I. Winey ¹

**Add the charles P. Easterling, ¹

Christopher C. Armstrong,

Karen I. Winey ¹

**Add the charles P. Easterling, ¹

Christopher C. Armstrong,

Charles P. Easterling, ²

Christopher C. Armstrong,

Charles P. Easterling, ³

Christopher C. Armstrong,

Charles P. Easterling,

Cha

We investigate a new series of precise ion-containing polyamide sulfonates (PASxLi), where a short polar block precisely alternates with a non-polar block of aliphatic carbons (x = 4, 5, 10, or 16) to form an alternating (AB)_n multiblock architecture. The polar block includes a lithiated phenyl sulfonate in the polymer backbone. These PASxLi polymers were synthesized via polycondensation of diaminobenzenesulfonic acid and alkyl diacids (or alkyl diacyl chlorides) with x-carbons, containing amide bonds at the block linkages. The para- and meta-substituted diaminobenzene monomers led to polymer analogs denoted pPASxLi and mPASxLi, respectively. When $x \le 10$, the para-substituted diamine monomer yields multiblock copolymers of a higher degree of polymerization than the meta-substituted isomer, due to the greater electron-withdrawing effect of the meta-substituted monomer. The PASxLi polymers exhibit excellent thermal stability with less than 5% mass loss at 300 °C and the glass transition temperatures ($T_{\rm o}$) decrease with increasing hydrocarbon block length (x). Using the random phase approximation, the Flory-Huggins interaction parameter (χ) is determined for pPAS10Li, and χ (260 °C) \sim 2.92 reveals high incompatibility between the polar ionic and non-polar hydrocarbon blocks. The polymer with the longest hydrocarbon block, pPAS16Li, is semicrystalline and forms well-defined nanoscale layers with a spacing of ~2.7 nm. Relative to previously studied polyester multiblock copolymers, the amide groups and aromatic rings permit the nanoscale layers to persist up to 250 °C and thus increase the stability range for ordered morphologies in precise ion-containing multiblock copolymers.

Received 22nd June 2022, Accepted 14th August 2022 DOI: 10.1039/d2py00802e

rsc.li/polymers

Introduction

Recent developments in polymer synthesis demonstrate the ability to control the periodicity of functional groups along a linear polymer backbone and obtain desired material properties. 1-4 Particularly, precise ion-containing multiblock copolymers have been synthesized with strictly alternating polar ionic blocks and non-polar hydrocarbon blocks of fixed lengths linked by ester groups.5-7 These ion-containing polyesters have high interaction parameter and chain architecture that enable self-assembly into morphologies with ordered ionic aggregates such as layered, double-gyroid, and hexagonally-packed cylinders. 6-8 Additionally, the modification of the polar ionic blocks and the hydrocarbon block lengths can control the ordered ionic aggregate morphologies. Specifically, double-gyroid morphologies persist over the composition window of ~14 vol% of the polar block.7 Recent studies with these precise ion-containing multiblock polyesters revealed that an ultrahigh Flory-Huggins interaction parameter (χ)

^aDepartment of Materials Science and Engineering, University of Pennsylvania, Philadelphia, Pennsylvania 19104, USA. E-mail: winey@seas.upenn.edu ^bCenter for Integrated Nanotechnologies, Sandia National Laboratories, Albuquerque, New Mexico 87185, USA

^cGeorge & Josephine Butler Polymer Research Laboratory, Center for Macromolecular Science & Engineering, Department of Chemistry, University of Florida, Gainesville, Florida 32611, USA

^dDepartment of Chemical and Biomolecular Engineering, University of Pennsylvania, Philadelphia, Pennsylvania 19104, USA

^eDepartment of Chemistry and Biochemistry, University of Maryland, College Park, Maryland 20742, USA. E-mail: mkt@umd.edu

[†] Electronic supplementary information (ESI) available: Synthesis of all polymers and 1 H NMR spectrum of mPAS4Li, pPAS4Li, mPAS5Li, and pPAS10Li. Infrared spectroscopy spectrum and X-ray scattering of pPAS16Li and its monomers. Chemistry of precise polyester sulfonates multiblock copolymers (PESxLi) and precise polyethylene with a phenyl sulfonate pendent to every 5th carbon (p5PhSA-Li). Thermogravimetric analysis. χ parameters of pPAS10Li at 230–260 °C. $In\ situ\ X$ -ray scattering of pPAS16Li. See DOI: https://doi.org/10.1039/d2py00802e

between the polar ionic and non-polar hydrocarbon blocks leads to the microphase separation at sub-3 nm length scales.⁸

The studies of precise ionomers show their potential as nanofabrication templates or ion transport membranes and motivate the synthesis of new multiblock chemistries to investigate the polymeric characteristics needed to design advanced precise ion-containing polymers.⁸⁻¹¹ Precise ion-containing multiblock copolymers are synthesized from the polycondensation reaction of two monomer species, each of fixed lengths. 5,12 For example, a sulfosuccinate diester block and an alkyl diol polymerize in a step-growth manner, where the length of the diol monomer determines the volume fraction of the polar block. Therefore, the chemistry of precise ion-containing multiblock copolymers with alternating sequences of polar ionic and non-polar blocks will be significantly expanded by further exploration of step-growth polymerizations. By using commercially available monomers, the straightforward modification of polar blocks can enhance the chemical and thermal stability relative to the precise ion-containing polyesters.

We selected polyamides as a promising platform to extend the chemistry of step-growth multiblock ionomers. Formed by the condensation of amines with carboxylic acids, polyamides comprise important biological polymers (e.g., peptides) and well-understood synthetic polymers (e.g., nylons). Thanks to decades of medicinal chemistry research into peptide formation, there are myriad known reactions to activate carboxylic acids towards nucleophilic attack by amines. 13,14 In addition to the well-established reaction conditions, polyamides also offer the significant advantage of commercially available building blocks. The reaction between the commercially available alkyl diacids (or even better, diacyl chlorides) and diamines makes possible the facile synthesis of structurally diverse polyamides, 15,16 leading to the design of polyamide ionomers with pendant sulfonate groups. 17-19 Polyamides tend to be highly crystalline due to the hydrogen bonding between amide groups, which are both H-bond donors and H-bond acceptors. Aromatic polyamides such as Kevlar are especially notable in this regard (with applications in bullet-proof vests and racing sails), 20 so we incorporated an aromatic ring into the ionic block of our targeted ionomers. Finally, polyamides are known for their excellent chemical and thermal stability. Amide bonds are more hydrolytically stable than ester linkages, making polyamides stable to a wider pH range than polyesters, and polyamides are known to withstand significantly higher temperatures than polyesters.²¹ This route can expand the structure-property relationships in precise ioncontaining multiblock copolymers.

In this paper, we report the synthesis and characterization of precise ion-containing polyamide lithium sulfonate multiblock copolymers (PASxLi) from the step-growth polymerization of benzenediamine sulfonates (*meta* or *para*-substituted) and alkyl diacids (or acyl chlorides) of a varying number of carbons (x). The polar blocks contain a single Li⁺SO₃⁻ group on the phenyl ring of the polymer backbone and alternate with short alkyl chains (x = 4-16). When x = 4, the degree of polymerization (n) of these (AB) $_n$ multiblock copolymers is

greater in *p*PAS4Li than *m*PAS4Li due to the poor nucleophilicity of the *meta*-substituted diamines. The presence of phenyl rings on the polymer backbone provides thermal stability up to ~300 °C in these PAS*x*Li polymers. The glass transition temperature (T_g) decreases with increasing x. X-ray scattering data reveals that the ion–ion correlation peak intensity of disordered ionic aggregates increases with x from 4 to 10. Unlike the semi-aromatic polyamides, $^{22-24}$ the presence of ionic groups on the phenyl ring prevents the crystallization of the hydrocarbon blocks with $x \le 10$. With a longer hydrocarbon block, pPAS16Li exhibits a semicrystalline polymer backbone and forms well-defined ionic layers with a spacing of ~2.7 nm. This work demonstrates the synthesis and characterization of new precise ion-containing polyamides that produce nanoscale ionic layers with great thermal stability.

Experimental section

Materials synthesis

See the ESI† for the detailed synthetic procedure of each polymer. All polymerization reactions were performed under an N₂ atmosphere using standard Schlenk techniques unless otherwise noted; polymer purifications and ion exchanges were performed under air. Chemical reagents were obtained from commercial vendors and used without further purification. Dialysis of polymer samples was performed using 7000 molecular weight cut-off (MWCO) regenerated cellulose dialysis tubing obtained from Sigma Aldrich. The final products were characterized by ¹H NMR on a Bruker Avance III 500 instrument at 298 K using a 5 mm broadband probe, with an observed frequency of 500.18 MHz.

Gel permeation chromatography (GPC)

GPC experiments were performed in *N*,*N*-dimethylacetamide (DMAc) with 50 mM LiCl at 50 °C and a flow rate of 1.0 mL min⁻¹ (Agilent isocratic pump, degasser, and autosampler; columns: Viscogel I-series 5 μ m guard + two ViscoGel I-series G3078 mixed bed columns, molecular weight range 0–20 × 10³ and 0–100 × 10⁴ g mol⁻¹). Detection consisted of a Wyatt Optilab T-rEX refractive index detector operating at 658 nm and a Wyatt miniDAWN Treos light scattering detector operating at 690 nm. All polymer samples were purified using 7K MWCO dialysis tubing before GPC measurements. Absolute molecular weights and molecular weight distributions of PAS materials were calculated using the Wyatt ASTRA software and dn/dc values obtained from 100% mass recovery. Due to the insolubility of *p*PAS16Li, the number of repeating units (*n*) of *p*PAS16Li was determined from *p*PAS16H.

Inductively coupled plasma optical emission spectroscopy (ICP-OES)

The content of Li in pPAS16Li was determined by ICP-OES using Genesis ICP, Spectro Analytical. A 10 mg of pPAS16Li was digested at 95 °C for 1 h in 5 mL of concentrated HNO $_3$ and 2 mL of H $_2$ O $_2$. Deionized water was added to a final

Polymer Chemistry Paper

volume of 50 mL. The standard deviation of Li content was determined from three replicates.

Thermal analysis

Thermogravimetric analysis (TGA) was performed with TA Instruments SDT Q600 under air with a flow rate of 100 mL min⁻¹. The weight change was recorded with an increasing temperature up to 480 °C and a 10 °C min⁻¹ ramping rate, after the equilibration for 5 min at 100 °C. Differential scanning calorimetry (DSC) experiments were performed with TA Instruments DSC2500 between 50 and 300 °C at a 10 °C min⁻¹ ramping rate under a nitrogen atmosphere. All samples were measured for two cycles of heating and cooling.

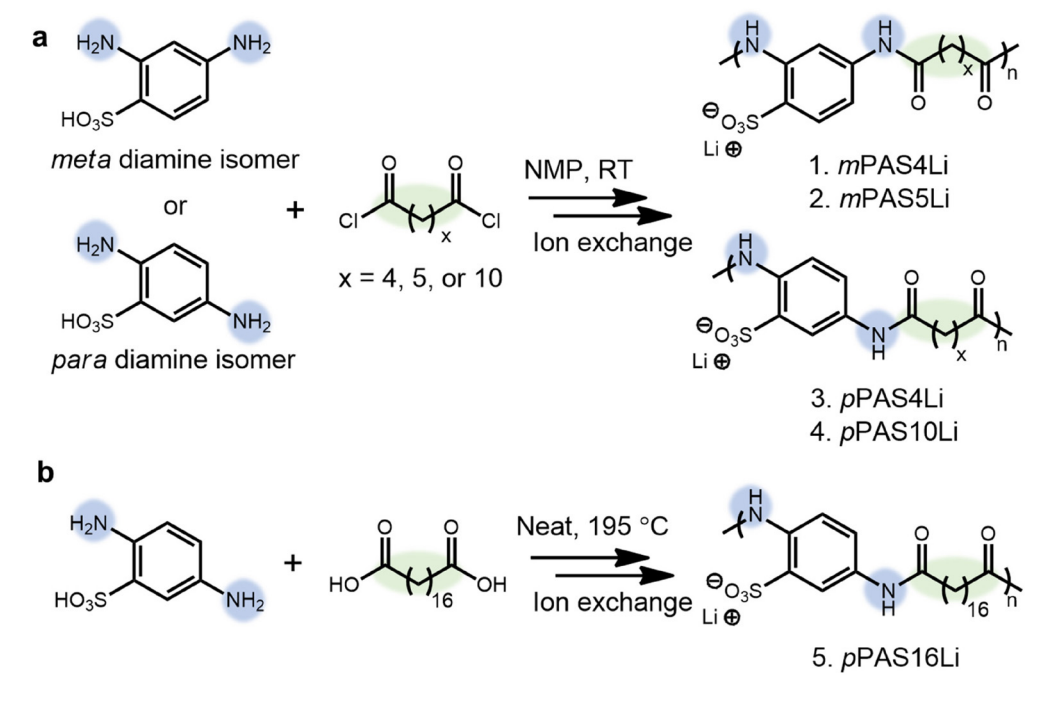
X-ray scattering experiments

X-ray scattering experiments were performed (Xeuss 2.0 from Xenocs) in the Dual-source and Environmental X-ray Scattering (DEXS) facility at the Laboratory for Research on the Structure of Matter, University of Pennsylvania. A PILATUS 1M detector and 100K detector were used for small-angle and wide-angle scattering, respectively. The sample to detector distance was ~370 mm and ~158 mm for the small- and wide-angle detectors, respectively. The beam source GeniX3D generates 8 keV Cu K α (wavelength ~ 1.54 Å). The 2D scattering data were collected at room temperature for 20 min. The X-ray scattering profiles of disordered pPAS10Li are collected for 20 min at 260-230 °C every 10 °C after an equilibration time of 10 min. In situ X-ray scattering profiles of pPAS16Li are collected for 10 min at 40-250 °C for every 10 °C upon heating with ramping at 10 °C min⁻¹ and equilibrating for 5 min. The scattering data were isotropic and integrated into I(q) plots. Smalland wide-angle I(q) plots were arbitrarily shifted to display the scattering data at 1 nm⁻¹ < q < 18 nm⁻¹.

Results and discussion

A library of polyamide ionomers was synthesized according to the routes shown in Scheme 1. To achieve mPAS4Li and mPAS5Li, 2,4-diaminobenzenesulfonic acid was reacted with adipoyl chloride or pimeloyl chloride, respectively, in a solution of N-methyl-2-pyrollidone (NMP) and diisopropylethylamine at room temperature. The polymerization yielded the diisopropylethylammonium salt of the desired polyamide sulfonate, so a series of ion exchanges were carried out in a solution of LiCl in NMP to yield the lithiated form of the polymer. Finally, the polymers were purified by aqueous dialysis and lyophilized to yield the pure products, mPAS4Li and mPAS5Li.

The yield for these two polymerizations was low: 6% for mPAS4Li and 19% for mPAS5Li. We hypothesized that the electron-withdrawing nature of the sulfonic acid group significantly hindered the nucleophilicity of the two aryl amines in 2,4-diaminobenzenesulfonic acid, since each amine is either ortho or para to the sulfonic acid. To enhance the nucleophilicity of the diamine monomer, we considered other isomers, in which the sulfonic acid group had less electronic communication with the amino groups. By reacting 2,5-diaminobenzenesulfonic acid with either adipoyl chloride or dodecanediol chloride under the same polymerization conditions described



Scheme 1 Synthesis of precise ion-containing polyamides were performed (a) in an NMP solution for mPAS4Li, mPAS5Li, pPAS4Li, and pPAS10Li, and (b) from the melt state for pPAS16Li.

Paper Polymer Chemistry

above, we obtained pPAS4Li and pPAS10Li, respectively. Gratifyingly, the yields for these reactions were significantly higher (53% for pPAS4Li and 28% for pPAS10Li). The 1 H NMR spectrum of all polymers in Scheme 1a is consistent with the expected amide, aromatic, and aliphatic protons (Fig. S1†). A diisopropylethylammonium cation was associated with the sulfonate groups in the first step of the synthesis, to solubilize the diaminobenzenesulfonic acid monomers. The absence of the diisopropylethylammonium peaks from the 1 H NMR spectra of the polymers indicated successful Li $^+$ exchange.

Encouraged by the improved nucleophilicity of 2,5-diaminobenzenesulfonic acid (para-substituted) in comparison to 2,4diaminobenzenesulfonic acid (meta-substituted), we targeted the synthesis of pPAS16Li with a longer alkyl spacer (x = 16). In this case, due to the lack of commercial availability of the diacyl chloride, we developed a new set of reaction conditions using 1,18-octadecanedioic acid. We found that by combining the two monomers neat and heating to 195 °C, the polymerization was able to proceed in the melt. 25,26 The solubility profile of pPAS16Li is distinct from that of the other polyamide ionomers reported here; pPAS16Li is insoluble in water, NMP, and LiCl/NMP (unlike the other lithiated PAS materials), likely due to the enhanced crystallinity of the longer alkyl block. Consequently, we were unable to obtain solution-state NMR spectra of pPAS16Li. Instead, the purified polymer was characterized by infrared spectroscopy and X-ray scattering, and these spectra were compared to data collected on the two monomers, 2,5-diaminobenzenesulfonic acid and octadecanedioic acid (Fig. S2 \dagger). In addition, the Li content of 1.66 \pm 0.031 wt% in pPAS16Li measured by the inductively coupled plasma optical emission spectroscopy agrees with the calculated Li content of 1.62 wt%, indicating the successful cation exchange. These results indicate the formation of the desired pPAS16Li shown in Scheme 1b, without residual monomer.

The absolute molecular weights of the PASxLi materials were determined from gel permeation chromatography (GPC) equipped with a light scattering detector. The molecular weights of *p*PAS4Li and *p*PAS10Li are significantly higher than those of the *meta* diamine isomers (Table 1), which we hypothesize to be a result of the higher nucleophilicity in *para*-substituted monomers than the *meta*-substituted diamine mono-

Table 1 Number-averaged molecular weight (M_n) and dispersity (D) for polyamide ionomer samples, as determined by gel permeation chromatography (GPC). The values of n represent the number of repeating units in these $(AB)_n$ alternating copolymers. The volume fraction of polar blocks (f_{polar}) is determined from the ratio of van der Waals volume

-				
Polymer	$M_{\rm n} \left({\rm g \ mol^{-1}} \right)$	Đ	n	$f_{ m polar}$
mPAS4Li	6260	1.48	20.6	0.71
mPAS5Li	5080	1.61	16.0	0.67
pPAS4Li	12 100	1.37	39.8	0.71
pPAS10Li	19 100	1.46	49.1	0.51
pPAS16H ^a	4420	1.43	9.46	0.40

 $[^]ap$ PAS16Li was sparingly soluble in the dimethylacetamide (0.05 M LiCl) solution used for GPC, so the $M_{\rm n}$ value was determined from the protonated form of the polymer, pPAS16H.

mers. The number-averaged molecular weight (M_n) of pPAS4Li is \sim 2 times larger than mPAS4Li at the same reaction condition. The GPC analysis for pPAS16Li was hindered by the poor solubility in the GPC solution (0.05 M LiCl in dimethylacetamide), and therefore the M_n of pPAS16Li was determined from the pPAS16H precursor (before cation exchange).

Thermal analysis of PAS materials

Thermogravimetric analysis (TGA) was performed to characterize the thermal stability of the PASxLi materials (Fig. 1). All polymer samples exhibit great thermal stability of less than 5% mass loss up to 300 °C, which is attributed to the presence of aromatic rings on the polymer backbones. We compared the thermal stability of PASxLi materials to other precise ion-containing sulfonates with lithium counter ions, in which the ionic group is also strictly segmented by the x-carbons spacer. See Fig. S3† for the block chemistries that we compare to PASxLi. 8,27 First, precise polyester sulfonates (PESxLi) containing a single Li⁺SO₃ group on the linear hydrocarbon backbone provide a comparison of backbone chemistry (aromatic vs. aliphatic). Both PES12Li and PES18Li exhibit ~50% mass loss at 300 °C, indicating the superior thermal stability of PASxLi materials relative to PES materials (Fig. S4†). Further, thermal stability decreases when the precise phenyl lithium sulfonates are located on the side chain of every 5th carbon (p5PhSA-Li),²⁷ rather than located on the polymer backbone as in the PASxLi materials. Thus, TGA results demonstrate the enhanced thermal stability of PASxLi materials in comparison to other precise ion-containing materials, due to the presence of phenyl lithium sulfonates in the polymer backbone.

Differential scanning calorimetry (DSC) was performed to characterize the thermal transition properties of the PASxLi polymers (Fig. 2). For mPAS4Li, mPAS5Li, and pPAS4Li, no thermal transitions are observed, indicating that the glass transition temperature (T_g) is inaccessible prior to polymer degra-

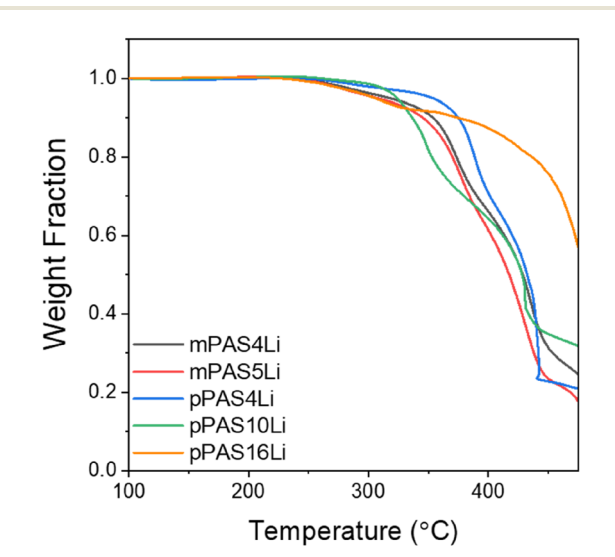


Fig. 1 Thermogravimetric analysis of the PASxLi polymers at a heating rate of 10 $^{\circ}$ C min $^{-1}$.

Polymer Chemistry Paper

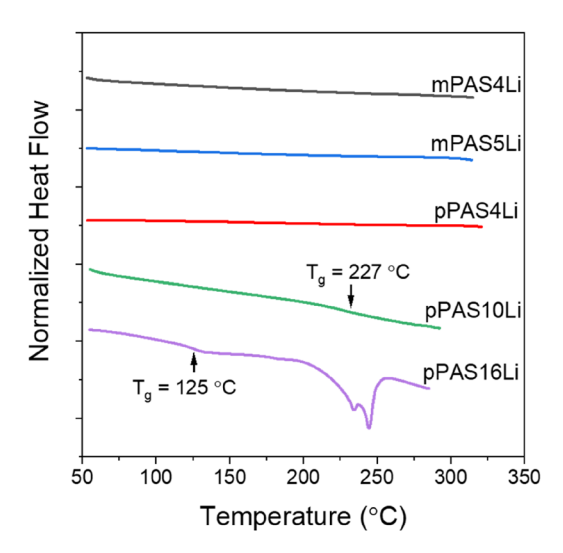


Fig. 2 The second heating of DSC traces (exo up) of the PAS polymers.

dation. In contrast, pPAS10Li, with a longer alkyl block and lower $f_{\rm polar}$, clearly shows a $T_{\rm g}\sim 227$ °C. With a further increase of the alkyl spacer, pPAS16Li exhibits a $T_{\rm g}\sim$ 125 °C and endothermic transition peaks at 235 °C and 243 °C. The decrease in T_g with a longer alkyl block length was also observed in PES materials, where the decrease in T_g was attributed to the decreased volume fraction of polar blocks and weaker electrostatic contributions to T_g . Thus, the decrease in T_g with a lower f_{polar} in PASxLi polymers is consistent with other precise ion-containing polymers. Note that the presence of rigid phenyl rings on the polymer backbone leads to a much higher T_g (~227 °C, $f_{\text{polar}} = 0.51$) in pPAS10Li compared to an analog with an aliphatic polyester backbone, PES12Li ($T_{\rm g}\sim$ 65 °C, $f_{\rm polar}=$ 0.41). Further, the T_g of pPAS10Li is higher than the semi-aromatic polyamide, poly(decamethylene terephthalamide), which has $T_{\rm g} \sim 133$ °C.²³ This indicates that the ionic groups of pPAS10Li contribute to increasing the polymer T_g , relative to the non-ionic and semi-aromatic polyamides.

PASxLi polymers with aliphatic carbon lengths of x = 4, 5,and 10 show no endothermic peaks in DSC traces, which indicates the absence of melting transitions. Note that the conventional aliphatic polyamide of nylon-6,6 exhibits the melting transition of ~270 °C.28 For PASxLi materials with shorter alkyl spacers ($x \le 10$), the absence of crystallization is attributed to the bulky ionic groups that hinder chain packing. The endothermic transitions of pPAS16Li are the result of longer hydrocarbon chain length and semicrystalline polymer backbones, which will be discussed in conjunction with the X-ray scattering experiments below. Although the crystallization requires a longer alkyl chain length, the transition temperatures in pPAS16Li are much higher than the melting transition in polyethylenes (~100-140 °C). 29,30

Morphology characterization of PASxLi materials

X-ray scattering data of PASxLi materials at room temperature were collected to investigate the correlations between polar

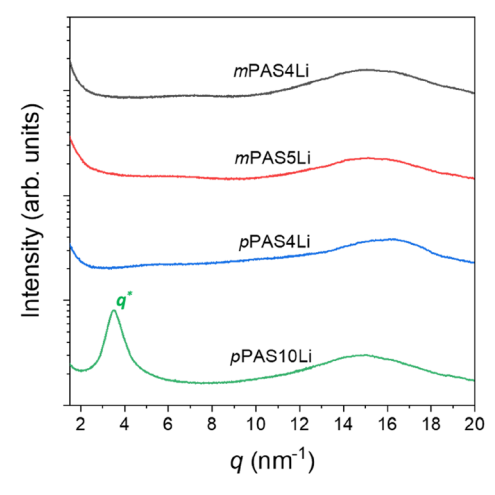


Fig. 3 X-ray scattering data of mPAS4Li, mPAS5Li, pPAS4Li, and pPAS10Li at room temperature.

blocks and the structures of the polymer backbone (Fig. 3). As indicated by a broad amorphous halo at $q \sim 15 \text{ nm}^{-1}$, the PASxLi polymers with $x \le 10$ are amorphous, which is consistent with the lack of melting transitions (Fig. 2). In contrast, the 12-carbon blocks of PES12Li crystallize with hexagonal packing.⁸ As the f_{polar} of pPAS10Li (0.51) is larger than the PES12Li (0.41), we conclude that the presence of bulkier polar blocks and rigid phenyl rings in pPAS10Li impede polymer crystallization. Therefore, X-ray scattering further indicates that PASxLi polymers with $x \le 10$ have alkyl blocks that are too short to allow crystalline chain packing. In polymers with short alkyl block lengths (x = 4, 5), no correlations between the polar blocks are detected, as indicated by the absence of peaks in the small-angle region ($q < 8 \text{ nm}^{-1}$). In contrast, pPAS10Li exhibits a correlation peak at $q^* \sim 3.5 \text{ nm}^{-1}$ that corresponds to 1.8 nm. We assign this peak to a disordered morphology, because the peak is broad and higher order peaks are absent.

It is useful to compare the extent of ion-ion correlations in PAS materials with other precise ion-containing polymers with various polar block chemistries. The p5PhSA-Li polymer produces disordered ionic aggregates with distinct ion-ion correlation peaks at $q^* \sim 3.2 \text{ nm}^{-1}$ and all-atom simulations have identified the percolated and stringy ionic aggregate structures. In contrast, PASxLi materials with x = 4 or 5 do not exhibit such ion-ion correlations. Therefore, the pendant ionic groups of p5PhSA-Li produce a greater degree of ionic aggregation relative to ionic groups embedded in the polymer backbone. Also, the chain flexibility of the polar blocks impacts the ionic aggregate morphologies.³² While the linear and aliphatic polar blocks in PES12Li assemble into layered ionic aggregates with the crystallization of hydrocarbon blocks, the reduced chain mobility of the rigid polar blocks in pPAS10Li hinders the formation of ionic aggregates. These comparisons of ionion correlations improve the understanding of how polar block chemistries impact the ionic aggregate morphologies in precise ion-containing multiblock copolymers.

Published on 23 August 2022. Downloaded by University of Pennsylvania Libraries on 5/22/2023 10:37:35 PM.

Paper Polymer Chemistry

Based on the disordered morphology of *p*PAS10Li, the effective Flory–Huggins interaction parameter (χ) of *p*PAS10Li was calculated using the random phase approximation for (AB)_n multiblock copolymers where the number of repeating units (n) > 20.^{33,34} The equation for fitting is provided in ESI.† Note that the absolute molecular weight of *p*PAS10Li determined from the GPC measurements corresponds to an *n* value of ~49. As the value of χ is inversely proportional to the reference volume, we normalized χ with a common reference volume of 0.118 nm^{3.35,36} The volume-based degree of polymerization is ~5.05, as calculated from the molecular

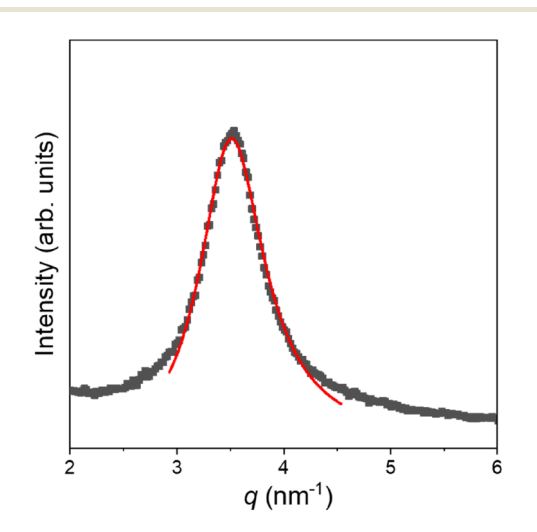


Fig. 4 Small-angle X-ray scattering data ($q < 6 \text{ nm}^{-1}$) of pPAS10Li at 260 °C and its fit (red line) to the random phase approximation theory of (AB)_n multiblock copolymers where $\chi = 2.92$ using the reference volume 118 nm³.

weight and density of melt polyethylene block, and the $f_{\rm polar}$ is ~0.51. The value of χ at 260 °C for pPAS10Li was determined to be 2.92 (Fig. 4), revealing the high incompatibility between the polar ionic and non-polar blocks. This value of χ for pPAS10Li is close to the χ at 260 °C for PES12Li ~ 3.10, which contains the same lithium sulfonate groups alternating with alkyl blocks and linked by ester groups. While χ values of block copolymers are usually inversely proportional to temperature, the χ values of pPAS10Li are insensitive to varying temperatures between 230–260 °C (Fig. S5†). A temperature-independent χ is also observed in ion-containing polystyrene-b-poly(ethylene oxide) and salt systems. 37

When the hydrocarbon block contains 16 carbons, pPAS16Li, X-ray scattering reveals well-defined ionic layers and a semicrystalline polymer backbone (Fig. 5a). The crystallization of the 16-carbon blocks is enabled by the exclusion of polar blocks from the crystals, presumably by chain folding of the polar block and similar to the chain conformation found in precise polyethylenes with acid functional groups. 9,38 A mixture of monoclinic and orthorhombic crystal structures is assigned to the wide-angle scattering peaks at $q > 12 \text{ nm}^{-1}$ and is consistent with previous reports of polyethylene-based ioncontaining polymers.^{5,39} The crystallization of hydrocarbon blocks in these multiblock copolymers produces layered ionic aggregate morphologies. Notably, we observe three layer-spacings corresponding to q_1^* , q_2^* , and q_3^* for pPAS16Li, that we attribute to the significant electron density difference between the Li⁺SO₃⁻ head-group (1640 nm⁻³), amide linkages (1140 nm⁻³), and hydrocarbon blocks (803 nm⁻³). The schematic in Fig. 5b illustrates the well-ordered ionic layers of pPAS16Li consisting of three distinct layers of the ionic groups (a), amide linkages (b), and hydrocarbon blocks (c) and stacked as abcba. The distance between the ionic layers

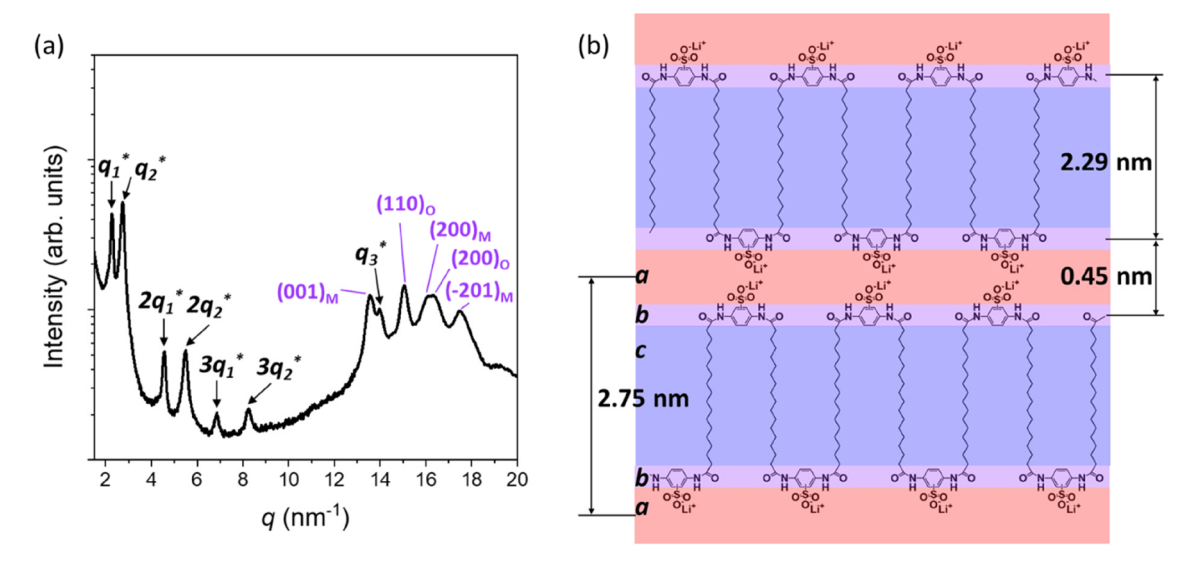


Fig. 5 (a) X-ray scattering of pPAS16Li at room temperature. (b) Schematic of chain conformations of pPAS16Li corresponding to the Bragg peaks at q_1^* , q_2^* , and q_3^* . The schematic shows the ionic groups, amide linkages, and the alkyl chains arranged in *abcba* stacks. The (hkl)_M and (hkl)_O correspond to the monoclinic and orthorhombic crystals of the hydrocarbon (16-carbon) blocks.

Polymer Chemistry Paper

Table 2 Summary of observed Bragg peak positions (q) in Fig. 5a from the abcba layered assembly and crystalline hydrocarbon blocks, and their real-space distances (d) at room temperature

		Hydrocarbon crystals			- 1 .1 .1 .43
q (nm ⁻¹)	d (nm)		$q (\mathrm{nm}^{-1})$	d (nm)	Polyethylene ⁴³ d (nm)
2.28	2.75	(001) _M	13.8	0.455	0.456
2.74	2.29		15.3	0.411	0.413
14.0	0.45	$(200)_{\mathbf{M}}$	16.4	0.384	0.384
	_	$(200)_{0}$	16.7	0.376	0.372
	_	$(-201)_{M}$	17.7	0.354	0.355
2	.28	.28 2.75 .74 2.29	$\begin{array}{cccccccccccccccccccccccccccccccccccc$	$ \begin{array}{cccccccccccccccccccccccccccccccccccc$	$ \begin{array}{c ccccccccccccccccccccccccccccccccccc$

 $(2\pi/q_1^*=2.75 \text{ nm})$ is the sum of distances of $2\pi/q_2^*=2.29 \text{ nm}$ and $2\pi/q_3^*=0.45 \text{ nm}$. Similarly, a trilayer structure has been observed in charged bottle-brush block copolymers. Also, trilayers of the crystalline triblock terpolymer exhibited similar X-ray scattering patterns. Also, and provides the corresponding spacings for the self-assembled layers and crystal structures. Note that the monoclinic and orthorhombic crystal structures assigned for pPAS16Li are consistent with established polyethylene crystal structures.

To explore the thermal and morphological transitions in pPAS16Li, $in \ situ \ X$ -ray scattering data were collected every 10 °C upon heating from 40 to 250 °C. Fig. 6 shows the intensity profile of pPAS16Li at 250 °C. Full scattering data are shown in Fig. S6.† The single peak at $q \sim 14.5 \ \mathrm{nm}^{-1}$ indicates the hexagonal symmetry of the polyethylene crystals, 44,45 which are also observed in the PES materials. 6,8 Therefore, the presence of hexagonal crystals in pPAS16Li at 250 °C reveals that the endothermic peaks in DSC (235 and 243 °C) traces shown in Fig. 2 correspond to transitions of crystal structures from monoclinic and orthorhombic to hexagonal symmetry, rather than a melting transition. In ion-containing polyethylenes, a higher melting transition than that of typical neat poly-

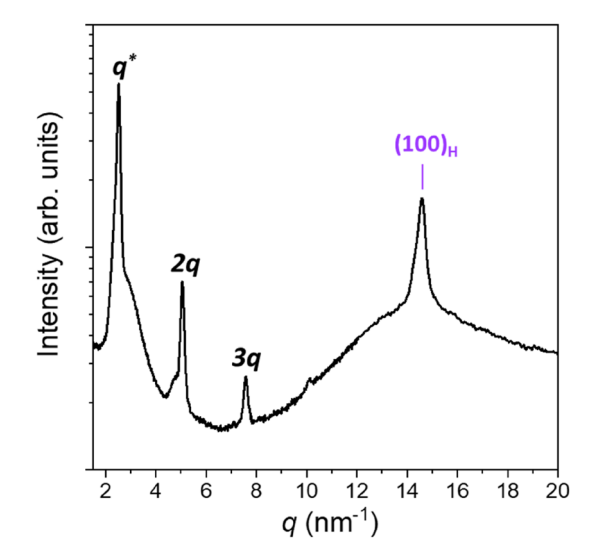


Fig. 6 X-ray scattering of pPAS16Li at 250 °C. The (100)_H indicates the hexagonal crystals of the polymer backbone.

ethylene is attributed to the strong association between the ionic groups, which impedes the melting of polyethylene crystals even though the crystals are small and poorly ordered. 39,46 The high melting temperature of pPAS16Li (>280 °C) is likely due to the strong electrostatic interaction between the polar ionic blocks, hydrogen bonding between the amide linkages, and the presence of aromatic rings in the polymer backbone. While X-ray scattering shows the abcba layered structure at room temperature, X-ray scattering at 250 °C shows a simpler ab layered structure. We attribute this difference to the thermal fluctuation of polar blocks that no longer exhibit a distinct electron density difference between the amide linkage and ionic head groups. As shown in Fig. S6,† the two distinct primary peaks ($q^* = 2.28$ and 2.74 nm⁻¹) present at 40 °C gradually merge upon heating to $q^* \sim 2.52 \text{ nm}^{-1}$ at 250 °C. While PESxLi polyesters with aliphatic polar blocks (x = 12-23) exhibit ordered ionic layers below 130 °C,6,8 pPAS16Li significantly extends accessible nanoscale ionic layers up to 250 °C.

Conclusions

This study explores precise ion-containing $(AB)_n$ multiblock copolymers with new block chemistries comprised of polyamide phenylsulfonates (PASxLi), in which the polar blocks and x-carbons alkyl blocks are strictly alternating. The structure of the diaminobenzene monomer was found to affect the polymer molecular weight, leading to a higher molecular weight for pPAS4Li (para-substituted monomer) than mPAS4Li (meta-substituted monomer). The presence of phenyl rings in the polymer backbone promotes thermal stability of the polymers, and all polymers exhibit less than 5% mass loss at 300 °C. The glass transition temperatures (T_g) of PASxLi materials with $x \le 5$ were inaccessible up to ~300 °C, while pPAS10Li and pPAS16Li exhibit $T_{\rm g}$ of ~227 and ~125 °C, respectively. The combination of amide groups and aromatic rings in the polymer backbone increases backbone rigidity that reduces ion-ion correlation for x = 4 and 5. When x = 10, X-ray scattering reveals a disordered morphology from which an interaction parameter for pPAS10Li was determined to be ~2.92, indicating an ultrahigh incompatibility between the polar and non-polar blocks. In pPAS16Li, the semicrystalline polymer backbone coexists with well-defined ionic layers with a spacing of ~2.7 nm. Compared to the previously studied

Paper

polyester multiblock copolymers, the nanoscale ionic layers of pPAS16Li persist up to 250 °C due to increased thermal stability. These PASxLi polymers expand the accessible block chemistries and provide insights to achieving ordered nanoscale morphologies in precise ion-containing $(AB)_n$ multiblock copolymers.

Conflicts of interest

There are no conflicts to declare.

Acknowledgements

J. P. and K. I. W. acknowledge the support of funding by the NSF DMR (1904767). J. P. and K. I. W. also acknowledge NSF MRSEC (17-20530), NSF MRI (17-25969), and ARO DURIP grant (W911NF-17-1-0282) for the Dual Source and Environmental Scattering facility the University at Pennsylvania. M. K. T. thanks the University of Maryland College Park for funding. This work was performed, in part, at the Center for Integrated Nanotechnologies, an Office of Science User Facility operated for the US DOE Office of Science. Sandia National Laboratories is a multimission laboratory managed and operated by National Technology and Engineering Solutions of Sandia, LLC, a wholly owned subsidiary of Honeywell International, Inc., for the US DOE's National Nuclear Security Administration (contract no. DE-NA-0003525). The views expressed in the article do not necessarily represent the views of the US DOE or the US government.

References

- 1 C. L. F. De Ten Hove, J. Penelle, D. A. Ivanov and A. M. Jonas, Encoding Crystal Microstructure and Chain Folding in the Chemical Structure of Synthetic Polymers, Nat. Mater., 2004, 3, 33-37.
- 2 P. Ortmann and S. Mecking, Long-Spaced Aliphatic Polyesters, Macromolecules, 2013, 46, 7213-7218.
- 3 P. Atallah, K. B. Wagener and M. D. Schulz, ADMET: The Future Revealed, Macromolecules, 2013, 46, 4735-4741.
- 4 L. Caire da Silva, G. Rojas, M. D. Schulz and K. B. Wagener, Acyclic Diene Metathesis Polymerization: History, Methods and Applications, Prog. Polym. Sci., 2017, 69, 79-107.
- 5 C. Rank, L. Yan, S. Mecking and K. I. Winey, Periodic Polyethylene Sulfonates from Polyesterification: Bulk and Nanoparticle Morphologies and Ionic Conductivities, Macromolecules, 2019, 52, 8466-8475.
- 6 L. Yan, C. Rank, S. Mecking and K. I. Winey, Gyroid and Other Ordered Morphologies in Single-Ion Conducting Polymers and Their Impact on Ion Conductivity, J. Am. Chem. Soc., 2020, 142, 857-866.
- 7 J. Park, A. Staiger, S. Mecking and K. I. Winey, Structure-Property Relationships in Single-Ion

- Multiblock Copolymers: A Phase Diagram and Ionic Conductivities, Macromolecules, 2021, 54, 4269-4279.
- 8 J. Park, A. Staiger, S. Mecking and K. I. Winey, Sub-3-Nanometer Domain Spacings of Ultrahigh-y Multiblock Copolymers with Pendant Ionic Groups, ACS Nano, 2021, **15**, 16738–16747.
- 9 E. B. Trigg, T. W. Gaines, M. Maréchal, D. E. Moed, P. Rannou, K. B. Wagener, M. J. Stevens and K. I. Winey, Self-Assembled Highly Ordered Acid Layers in Precisely Sulfonated Polyethylene Produce Efficient Transport, Nat. Mater., 2018, 17, 725-731.
- 10 J. Park, A. Staiger, S. Mecking and K. I. Winey, Ordered Nanostructures in Thin Films of Precise Ion-Containing Multiblock Copolymers, ACS Cent. Sci., 2022, 8, 388-393.
- 11 J. Park, A. Staiger, S. Mecking and K. I. Winey, Enhanced Li-Ion Transport through Selectively Solvated Ionic Layers of Single-Ion Conducting Multiblock Copolymers, ACS Macro Lett., 2022, 11, 1008-1013.
- 12 L. Yan, L. Hoang and K. I. Winey, Ionomers from Step-Growth Polymerization: Highly Ordered Ionic Aggregates and Ion Conduction, Macromolecules, 2020, 53, 1777-1784.
- 13 C. A. G. N. Montalbetti and V. Falque, Amide Bond Formation and Peptide Coupling, Tetrahedron, 2005, 61, 10827-10852.
- 14 R. M. Lanigan and T. D. Sheppard, Recent Developments in Amide Synthesis: Direct Amidation of Carboxylic Acids and Transamidation Reactions, Eur. J. Org. Chem., 2013, 7453-7465.
- 15 J. M. García, F. C. García, F. Serna and J. L. de la Peña, High-Performance Aromatic Polyamides, Prog. Polym. Sci., 2010, 35, 623-686.
- 16 K. Marchildon, Polyamides Still Strong after Seventy Years, Macromol. React. Eng., 2011, 5, 22-54.
- 17 A. Molnár and A. Eisenberg, Miscibility of Polyamide-6 with Lithium or Sodium Sulfonated Polystyrene Ionomers, Macromolecules, 1992, 25, 5774-5782.
- 18 S. Viale, W. F. Jager and S. J. Picken, Synthesis and Characterization of a Water-Soluble Rigid-Rod Polymer, Polymer, 2003, 44, 7843-7850.
- 19 Y. Wang, Y. He, Z. Yu, J. Gao, S. ten Brinck, C. Slebodnick, G. B. Fahs, C. J. Zanelotti, M. Hegde, R. B. Moore, B. Ensing, T. J. Dingemans, R. Qiao and L. A. Madsen, Double Helical Conformation and Extreme Rigidity in a Rodlike Polyelectrolyte, Nat. Commun., 2019, 10, 1-8.
- 20 J. A. Reglero Ruiz, M. Trigo-López, F. C. García and J. M. García, Functional Aromatic Polyamides, Polymers, 2017, 9, 414.
- 21 P. Ranganathan, C. W. Chen, S. P. Rwei, Y. H. Lee and S. K. Ramaraj, Methods of Synthesis, Characterization and Biomedical Applications of Biodegradable Poly(Ester Amide)s - A Review, Polym. Degrad. Stab., 2020, 181, 109323.
- 22 A. J. Uddin, Y. Ohkoshi, Y. Gotoh, M. Nagura, R. Endo and T. Hara, Melt Spinning and Laser-Heated Drawing of a New Semiaromatic Polyamide, PA9-T Fiber, J. Polym. Sci., Part B: Polym. Phys., 2004, 42, 433-444.

- 23 W. Wang, X. Wang, R. Li, B. Liu, E. Wang and Y. Zhang, Environment-Friendly Synthesis of Long Chain Semiaromatic Polyamides with High Heat Resistance Wenzhi, J. Appl. Polym. Sci., 2009, 114, 2036–2042.
- 24 S. H. Yang, P. Fu, M. Y. Liu, Y. D. Wang, Y. C. Zhang and Q. X. Zhao, Synthesis, Characterization of Polytridecamethylene 2,6-Naphthalamide as Semiaromatic Polyamide Containing Naphthalene-Ring, eXPRESS Polym. Lett., 2010, 4, 442–449.
- 25 C. Bennett and L. J. Mathias, Synthesis and Characterization of Polyamides Containing Octadecanedioic Acid: Nylon-2,18, Nylon-3,18, Nylon-4,18, Nylon-6,18, Nylon-8,18, Nylon-9,18, and Nylon-12,18, *J. Polym. Sci., Part A: Polym. Chem.*, 2005, 43, 936–945.
- 26 C. Bennett, E. Kaya, A. M. Sikes, W. L. Jarrett and L. J. Mathias, Synthesis and Characterization of Nylon 18 18 and Nylon 18 Adamantane, J. Polym. Sci., Part A: Polym. Chem., 2009, 47, 4409–4419.
- 27 A. Kendrick, W. J. Neary, J. D. Delgado, M. Bohlmann and J. G. Kennemur, Precision Polyelectrolytes with Phenylsulfonic Acid Branches at Every Five Carbons, *Macromol. Rapid Commun.*, 2018, 39, 1–7.
- 28 C. Ramesh, A. Keller and S. J. E. A. Eltink, Studies on the Crystallization and Melting of Nylon 66: 3. Melting Behaviour of Negative Spherulites by Calorimetry, *Polymer*, 1994, 35, 5300–5308.
- 29 P. J. Flory and A. Vrij, Melting Points of Linear-Chain Homologs. The Normal Paraffin Hydrocarbons, *J. Am. Chem. Soc.*, 1963, **85**, 3548–3553.
- 30 R. G. Alamo, B. D. Viers and L. Mandelkern, A Re-Examination of the Relation between the Melting Temperature and the Crystallization Temperature: Linear Polyethylene, *Macromolecules*, 1995, **28**, 3205–3213.
- 31 B. A. Paren, B. A. Thurston, W. J. Neary, A. Kendrick, J. G. Kennemur, M. J. Stevens, A. L. Frischknecht and K. I. Winey, Percolated Ionic Aggregate Morphologies and Decoupled Ion Transport in Precise Sulfonated Polymers Synthesized by Ring-Opening Metathesis Polymerization, *Macromolecules*, 2020, 53, 8960–8973.
- 32 J. Park and K. I. Winey, Double Gyroid Morphologies in Precise Ion-Containing Multiblock Copolymers Synthesized via Step-Growth Polymerization, *JACS Au*, 2022, DOI: 10.1021/jacsau.2c00254.
- 33 H. Benoit and G. Hadziioannou, Scattering Theory and Properties of Block Copolymers with Various Architectures in the Homogeneous Bulk State, *Macromolecules*, 1988, 21, 1449–1464.
- 34 L. Wu, E. W. Cochran, T. P. Lodge and F. S. Bates, Consequences of Block Number on the Order-Disorder Transition and Viscoelastic Properties of Linear $(AB)_n$

- Multiblock Copolymers, *Macromolecules*, 2004, 37, 3360-3368
- 35 C. Sinturel, F. S. Bates and M. A. Hillmyer, High χ-Low N Block Polymers: How Far Can We Go?, *ACS Macro Lett.*, 2015, **4**, 1044–1050.
- 36 N. Hampu and M. A. Hillmyer, Molecular Engineering of Nanostructures in Disordered Block Polymers, *ACS Macro Lett.*, 2020, **9**, 382–388.
- 37 W. S. Loo, G. K. Sethi, A. A. Teran, M. D. Galluzzo, J. A. Maslyn, H. J. Oh, K. I. Mongcopa and N. P. Balsara, Composition Dependence of the Flory-Huggins Interaction Parameters of Block Copolymer Electrolytes and the Isotaksis Point, *Macromolecules*, 2019, 52, 5590–5601.
- 38 E. B. Trigg, M. J. Stevens and K. I. Winey, Chain Folding Produces a Multilayered Morphology in a Precise Polymer: Simulations and Experiments, *J. Am. Chem. Soc.*, 2017, **139**, 3747–3755.
- 39 A. Staiger, B. A. Paren, R. Zunker, S. Hoang, M. Häußler, K. I. Winey and S. Mecking, Anhydrous Proton Transport within Phosphonic Acid Layers in Monodisperse Telechelic Polyethylenes, J. Am. Chem. Soc., 2021, 143, 16725–16733.
- 40 J. Shim, F. S. Bates and T. P. Lodge, Superlattice by Charged Block Copolymer Self-Assembly, *Nat. Commun.*, 2019, **10**, 1–7.
- 41 J. K. Palacios, A. Tercjak, G. Liu, D. Wang, J. Zhao, N. Hadjichristidis and A. J. Müller, Trilayered Morphology of an ABC Triple Crystalline Triblock Terpolymer, *Macromolecules*, 2017, **50**, 7268–7281.
- 42 J. K. Palacios, G. Liu, D. Wang, N. Hadjichristidis and A. J. Müller, Generating Triple Crystalline Superstructures in Melt Miscible PEO-b-PCL-b-PLLA Triblock Terpolymers by Controlling Thermal History and Sequential Crystallization, Macromol. Chem. Phys., 2019, 220, 1–14.
- 43 K. E. Russell, B. K. Hunter and R. D. Heyding, Monoclinic Polyethylene Revisited, *Polymer*, 1997, **38**, 1409–1414.
- 44 S. Tsubakihara, A. Nakamura and M. Yasuniwa, Hexagonal Phase of Polyethylene Fibers under High Pressure, *Polym. J.*, 1991, 23, 1317–1324.
- 45 K. Tashiro, S. Sasaki and M. Kobayashi, Structural Investigation of Orthorhombic-to-Hexagonal Phase Transition in Polyethylene Crystal: The Experimental Confirmation of the Conformationally Disordered Structure by X-Ray Diffraction and Infrared/Raman Spectroscopic Measurements, Macromolecules, 1996, 29, 7460–7469.
- 46 H. Steininger, M. Schuster, K. D. Kreuer, A. Kaltbeitzel, B. Bingöl, W. H. Meyer, S. Schauff, G. Brunklaus, J. Maier and H. W. Spiess, Intermediate Temperature Proton Conductors for PEM Fuel Cells Based on Phosphonic Acid as Protogenic Group: A Progress Report, *Phys. Chem. Chem. Phys.*, 2007, 9, 1764–1773.